The impact of $h \to Z\gamma$ in models with two scalar doublets (Extended Abstract)

Duarte Fontes (n. 67909)
Departamento de Física, Instituto Superior Técnico, Universidade de Lisboa, Lisboa, Portugal
(Dated: October 17, 2014)

There is already an upper bound for $h \to Z\gamma$ and an observation might be feasible at the upcoming LHC run. We perform a complete evaluation of that process in the most general model with two Higgs doublets and softly broken symmetry Z_2, where the Higgs-like particle could be a mixture of a scalar and a pseudoscalar components. We show that in all the four versions of this model a large pseudoscalar component is already disfavoured at 1-σ. We analyze the wrong sign $h\bar{b}b$ Yukawa coupling both in the CP conserving and in the CP violating models.

I. INTRODUCTION

Since the discovery of a scalar neutral particle in 2012 with a mass close to 125 GeV confirmed by the ATLAS [1] and CMS [2] collaborations from the LHC, the search for a deeper understanding on the Higgs physics has gathered attentions all over the world. The CDF and D0 collaborations from FermiLab [3, 4] provided additional evidence on the discovery, and recent announcements made both by ATLAS [5] and CMS [6] leave no doubt regarding the confirmation of such a particle[1].

The scalar particle has been discovered through its decays to $\gamma\gamma$, ZZ^*, WW^* and $\tau^+\tau^-$ with errors of order 20% (the several decay modes are presented in Figure 1). Decays into $b\bar{b}$ are only detected at LHC and the Tevatron in connection with the associated Vh production mechanism, with errors of order 50% [7, 8]. The experimental results for $pp \to h \to f$ (where p represents a proton, h the Higgs and f some final state) are usually presented in the form of ratios of observed rates to Standard Model (SM) expectations, which we call μ_f.

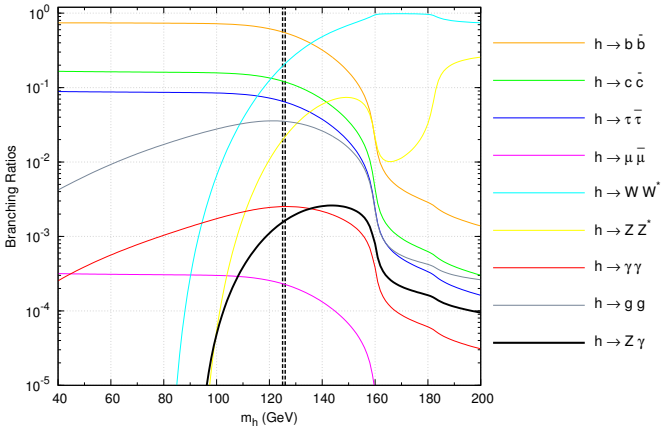

FIG 1. The Branching Ratios of the Higgs decays. The mass of the recently discovered scalar is marked with a dotted line.

The SM therefore corresponds to $\mu_f = 1 \ \ \forall f$. For definiteness, our discussions will be based on the ATLAS [9] and CMS [10] results presented in the plenary talks at ICHEP2014, which we summarize in Table 1.

channel	ATLAS	CMS
$\mu_{\gamma\gamma}$	$1.57^{+0.33}_{-0.28}$	1.13 ± 0.24
μ_{WW}	$1.00^{+0.32}_{-0.29}$	0.83 ± 0.21
μ_{ZZ}	$1.44^{+0.40}_{-0.35}$	1.00 ± 0.29
$\mu_{\tau^+\tau^-}$	$1.4^{+0.5}_{-0.4}$	0.91 ± 0.27
$\mu_{b\bar{b}}$	$0.2^{+0.7}_{-0.6}$	0.93 ± 0.49

TABLE 1. Experimental results presented by ATLAS and CMS at ICHEP2014.

We note that ATLAS excludes the SM $\mu_{\gamma\gamma} = 1$ ($\mu_{ZZ} = 1$) at 2-σ (1-σ), while CMS is within 1-σ of the SM on all channels. The discovered scalar is thus compatible with the SM Higgs boson (an interval of 2-σ is not sufficient to declare incompatibility). However, such an identification as the SM Higgs boson is not certain yet[2]; indeed, from Table 1 we see that ATLAS shows a small excess of observed events in the $h \to \gamma\gamma$ channel. One possible explanation for such an excess considers additional charged particles contributing to the loop which mediates the decay: such charged particles would participate at the same perturbative order as those of the SM, making this decay a very sensitive one to new physics. In such a scenario, another related decay for which the new charged particles would also contribute is the $h \to Z\gamma$. Therefore, and despite being highly suppressed decays (see Fig. 1), the $h \to \gamma\gamma$ and $h \to Z\gamma$ processes might be preponderant in our understanding into possible Beyond the SM (BSM) models.

The $h \to \gamma\gamma$ decay, having been one of the channels through which the new particle has been discovered, has

[1] This discovery has been an extraordinary success, since both the dominant production cross section (gluon-gluon fusion) and the main channel of detection ($\gamma\gamma$) occur only at 1 loop.

[2] Nevertheless, we shall henceforth refer to the newfound particle as a/the Higgs boson; the question which remains open is whether the discovered Higgs boson is unique and identical to the one predicted by the SM, h.

already been studied using experimental data (see, for example, Refs. [11–13]). The $h \to Z\gamma$ channel, on the other hand, has not yet been observed, although there already exists an upper bound. These results will be enhanced in the future 14 TeV LHC run, establishing this decay as one of the very next experimental goals.

One of the simplest extensions to the SM considers not one but two Higgs doublets, while keeping the remaining particle content and the symmetries of the model intact. It is the so-called 2 Higgs Doublet Model (2HDM) [16], which naturally accommodates extra charged particles and therefore provides an appealing scenario for the aforementioned excess of observed events. The 2HDM can be separated in two major branches: the CP conserving 2HDM (also known as real 2HDM, or simply 2HDM) and the CP violating 2HDM (also known as Complex 2HDM, or C2HDM). The latter appears as an attempt to answer the question of whether the newfound particle has some pseudoscalar component. In each of the two models, we calculate the $h \to Z\gamma$ decay width at one loop and we compare it with the one in the SM. As the new models introduce new parameters, we investigate the region of the parameter space which is still available for the models, given the current bounds imposed by the experiments.

Recently, the ATLAS and CMS collaborations have started ascertaining the values of the couplings between the Higgs and the fermions [17, 18]. It has recently been emphasized by Carmi et al. [19], by Chiang and Yagyu [20], by Santos [21] and by Ferreira et al. [22] that current data are consistent with a lightest Higgs from a 2HDM in which the coupling of the bottom quark to that Higgs particle ($hb\bar{b}$) has a sign *opposite* to that in the SM. We study this possibility both in the 2HDM as in the C2HDM, emphasizing the role of the $h \to Z\gamma$.

II. MODEL AND SIMULATION

We consider a model with two Higgs doublets, Φ_1 and Φ_2, with softly broken symmetry Z_2. The the most general potential obeying the requirements of hermiticity, $SU(2) \times U(1)$ gauge symmetry and renormalizability is

$$\begin{aligned} V =& m_{11}^2 \Phi_1^\dagger \Phi_1 + m_{22}^2 \Phi_2^\dagger \Phi_2 - \left(m_{12}^2 \Phi_1^\dagger \Phi_2 + h.c. \right) + \\ & \frac{\lambda_1}{2} \left(\Phi_1^\dagger \Phi_1 \right)^2 + \frac{\lambda_2}{2} \left(\Phi_2^\dagger \Phi_2 \right)^2 + \lambda_3 \Phi_1^\dagger \Phi_1 \Phi_2^\dagger \Phi_2 \\ & + \lambda_4 \Phi_1^\dagger \Phi_2 \Phi_2^\dagger \Phi_1 + \left[\frac{\lambda_5}{2} \left(\Phi_1^\dagger \Phi_2 \right)^2 + h.c. \right], \end{aligned} \tag{1}$$

where m_{12}^2 and λ_5 are in general complex, while the remaining parameters are real. There is only CP violation if $\arg(\lambda_5) \neq 2\arg(m_{12}^2)$. If this relation holds, the resulting model is the C2HDM. If, however, the relation is not verified, then we can always choose a basis where m_{12}^2 and λ_5 are real and, if the vacuum expectations values (vevs) are also real, then we get the special case of the real 2HDM.

The parametrization of the doublets after the spontaneous symmetry breaking might be given by [23]:

$$\Phi_1 = \begin{pmatrix} \phi_1^+ \\ \dfrac{v_1 + \eta_1 + i\chi_1}{\sqrt{2}} \end{pmatrix}, \quad \Phi_2 = \begin{pmatrix} \phi_2^+ \\ \dfrac{v_2 + \eta_2 + i\chi_2}{\sqrt{2}} \end{pmatrix}, \tag{2}$$

where η_i and χ_i represent the real and imaginary parts of the neutral scalar fields. The physical fields are obtained using the angle β which is such that $\tan\beta := v_2/v_1$:

$$\begin{aligned} H^\pm &= -s_\beta \phi_1^\pm + c_\beta \phi_2^\pm, & G^\pm &= c_\beta \phi_1^\pm + s_\beta \phi_2^\pm, \\ \eta_3 &= -s_\beta \chi_1 + c_\beta \chi_2, & G^0 &= c_\beta \chi_1 + s_\beta \chi_2, \end{aligned} \tag{3}$$

where $s_\beta = \sin\beta$, $c_\beta = \cos\beta$. The three neutral fields η_1, η_2 and η_3 are mixed together, so that the physical states h_1, h_2 and h_3 are obtained from them through the relation [24]

$$\begin{pmatrix} h_1 \\ h_2 \\ h_3 \end{pmatrix} = \begin{pmatrix} c_1 c_2 & s_1 c_2 & s_2 \\ -(c_1 s_2 s_3 + s_1 c_3) & c_1 c_3 - s_1 s_2 s_3 & c_2 s_3 \\ -c_1 s_2 c_3 + s_1 s_3 & -(c_1 s_3 + s_1 s_2 c_3) & c_2 s_3 \end{pmatrix} \begin{pmatrix} \eta_1 \\ \eta_2 \\ \eta_3 \end{pmatrix}, \tag{4}$$

where we have introduced the angles α_i and defined $s_i \equiv \sin(\alpha_i)$ and $c_i \equiv \cos(\alpha_i)$ $(i = 1, 2, 3)$. As input parameters of the potential, we choose the set [24]

$$\left\{ m_1,\ m_2,\ m_{H^\pm},\ \alpha_1,\ \alpha_2,\ \alpha_3,\ \beta,\ \mathrm{Re}\left(m_{12}^2\right) \right\}, \tag{5}$$

where $m_j = m_{h_j}$. We shall assume the relation $m_1 \leq m_2 \leq m_3$. The value of m_3 can be calculated from this set.

We assume that the SM particles except the Higgs follow the usual Lagrangian, that there are $H^\pm$ particles with the usual gauge-kinetic Lagrangian, and that the 125 GeV scalar/pseudoscalar particle h has the following interactions with the fermions, the charged Higgs boson and the vectorial gauge bosons:

$$\mathcal{L}_Y = -\left(\sqrt{2} G_F\right)^{\frac{1}{2}} m_f\ \bar{\psi} \left(a + i b \gamma_5\right) \psi\, h, \tag{6}$$

$$\mathcal{L}_{hH^+H^-} = \lambda\, v\, h H^+ H^-, \tag{7}$$

$$\mathcal{L}_{hVV} = C \left[g\, m_W W_\mu^+ W^{\mu-} + \frac{g}{2c_W} m_Z Z_\mu Z^\mu \right] h, \tag{8}$$

where $VV = ZZ^*$ or W^+W^-, and where a, b, C and λ are real parameters. The specification of these parameters defines the model. The C2HDM corresponds to the set of parameters given in Ref. [25] (and one should identify h with h_1), where the choice of the different pairs of values a and b for each fermion defines the version of the model. There are four of them: Type I, Type II, Lepton Specific and Flipped. The CP conserving 2HDM has $b = 0$ and a, C and λ given in Ref. [26]. In this case, we also have $\alpha_2 = \alpha_3 = 0$ and use α instead of α_1, such that $\alpha = \alpha_1 - \frac{\pi}{2}$. In the special case of the SM, one simply has $a = C = 1$ and $b = \lambda = 0$.

We use the ratios of observed rates to SM expectations to constrain the ratios between the 2HDM and SM rates

$$\mu_f = R_P\, R_D\, R_{TW}, \tag{9}$$

where the sub-indices P, D, and TW stand for "production", "decay", and "total width", respectively. Here,

$$R_P = \frac{\sigma^{\rm 2HDM}(pp \to h)}{\sigma^{\rm SM}(pp \to h)},$$

$$R_D = \frac{\Gamma^{\rm 2HDM}[h \to f]}{\Gamma^{\rm SM}[h \to f]},$$

$$R_{TW} = \frac{\Gamma^{\rm SM}[h \to \text{all}]}{\Gamma^{\rm 2HDM}[h \to \text{all}]}, \tag{10}$$

where σ is the Higgs production mechanism, $\Gamma[h \to f]$ the decay width into the final state f, and $\Gamma[h \to \text{all}]$ is the total Higgs decay width.

For our simulations, we generate points in parameter space with $m_1 = 125$ GeV and with the ranges

$$\alpha_1 \in \left[-\frac{\pi}{2}, \frac{\pi}{2}\right], \qquad \alpha_2 \in \left[-\frac{\pi}{2}, \frac{\pi}{2}\right], \qquad \alpha_3 \in \left[0, \frac{\pi}{2}\right],$$

$$\tan\beta \in [1, 30], \qquad m_2 \in [125, 900]\ \text{GeV},$$

$$m_{H^\pm} \in [340, 900]\ \text{GeV (Type II and Flipped)},$$

$$m_{H^\pm} \in [100, 900]\ \text{GeV (Type I and Lepton Specific)},$$

$$m_{12}^2 \in \left[-900^2, 900^2\right]\ \text{GeV}^2.$$

We only maintain those points which provide a bounded from below solution [27], conforming to perturbative unitarity [28] and the oblique radiative parameters S, T, U [29, 30]. After implementing this algorithm, we have a collection of possible C2HDM data points.

It can be shown that η_1 and η_2 are scalars fields and η_3 is pseudoscalar. Using the fact that there is CP violation when a certain field has a scalar and a pseudoscalar component and also Eq. 4, one can see that, if $s_2 = 0$, h_1 becomes a function of η_1 and η_2 only, so that it is a pure scalar. In the case $|s_2| = 1 \Leftrightarrow c_2 = 0$, we have that $h_1 = h_1(\eta_3)$, so that h_1 is a pure pseudoscalar. This seems to imply that $|s_2|$ is a good measure of the pseudoscalar content of h_1. Therefore, to study the effect of current experimental bounds on the pseudoscalar content of the 125 GeV Higgs, we follow Ref. [12] and study three sets of points: points where the h_1 is mainly scalar, with $|s_2| < 0.1$ (in green/light-grey in the simulation figures to be shown below); points where the h_1 is mainly pseudoscalar, with $|s_2| > 0.85$ (in red/dark-grey in the simulation figures to be shown below); points where the h_1 is a almost even mix of scalar and pseudoscalar, with $0.45 < |s_2| < 0.55$ (in blue/black in the simulation figures to be shown below). To compare with current experiments, all scatterplots in this article will be drawn for processes at 8 TeV, except were noted otherwise.

For the study of the wrong-sign Yukawa coupling, we concentrate mostly on the Type II 2HDM. In fact, given the experimental lower bound on $\tan\beta$, the coupling to the up-type quarks in Type I and Type II - as well as the coupling to the down-type quarks in Type I - cannot have the wrong sign [22]. We will use the notation k_U and k_D for the values of a related to the up-type quarks and the down-type quarks in Type II real 2HDM, respectively. We have [26]:

$$k_U = \frac{g_{hUU}^{\rm Type\ II}}{g_{hUU}^{\rm SM}} = \frac{\cos(\alpha)}{\sin(\beta)}, \qquad k_D = \frac{g_{hDD}^{\rm Type\ II}}{g_{hDD}^{\rm SM}} = -\frac{\sin(\alpha)}{\cos(\beta)}, \tag{11}$$

and $\sin\alpha$ is such that

$$\sin(\alpha) < 0 \quad \Rightarrow \quad k_D > 0 \quad \Leftrightarrow \quad \text{SM sign},$$

$$\sin(\alpha) > 0 \quad \Rightarrow \quad k_D < 0 \quad \Leftrightarrow \quad \text{opposite sign}\ .$$

III. THE $h \to Z\gamma$ DECAY

The $h \to Z\gamma$ decay does not happen at tree level, since the photon does not couple to electrically neutral particles. We thus focus on the decay at one loop. In a general 2HDM, we can have three sorts of diagrams mediating the loop: fermions, vectorial bosons and charged scalars. We present in Figs. 2, 3 and 4 examples of these diagrams.

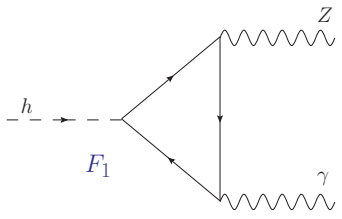

FIG 2. Fermion mediated loop diagram.

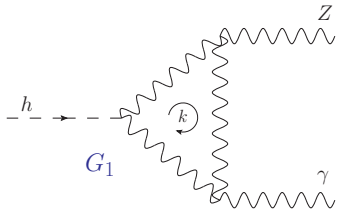

FIG 3. Vectorial boson mediated loop diagram.

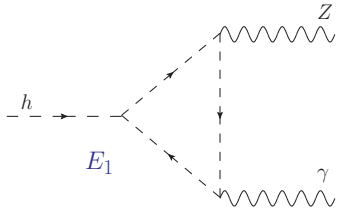

FIG 4. Scalar mediated loop diagram.

If Y_F and Ψ_F represent dimensionless functions related to the scalar and pseudoscalar contributions from the fermion mediated loop diagrams for the final decay width, respectively, and if Y_G and Y_H are the analogous scalar contributions from the vectorial bosons and charged scalars, respectively, then it can be shown that the decay width can be written as [25]

$$\Gamma(h \to Z\gamma) = \frac{G_F \alpha^2 m_h^3}{64\sqrt{2}\pi^3}\left(1 - \frac{m_Z^2}{m_h^2}\right)^3 \left(|a\, Y_F + C\, Y_G + \lambda Y_H|^2 + |\Psi_F|^2\right) . \quad (12)$$

Two points should be stressed: first, although some individual amplitudes might not be, the final result is finite and gauge invariant, which we have checked with `Feyncalc` [31]; second, from Eq. 12, we see that there is no interference between the scalar and the pseudoscalar components.

IV. RESULTS AND DISCUSSION

i. Squared moduli inside $\Gamma(h \to Z\gamma)$

We present in Fig. 5 a scatterplot comparing the squared moduli of the different terms in Eq. 12, where we are taking $X_W = C\, Y_G$, $X_t = k_U\, Y_{F\,\mathrm{top}}$, $X_b = k_D\, Y_{F\,\mathrm{bottom}}$ and $X_{H^\pm} = \lambda\, Y_H$ (we have considered independently the top and bottom quarks contributions). The squared moduli have been computed in the Type II 2HDM with both $k_D < 0$ and $k_D > 0$. The diagrams mediated by internal vectorial bosons have the most expressive contribution. The charged Higgs contribution is non-negligible, being comparable to the top quark one. The pseudoscalar contributions, Ψ_t and Ψ_b, relative to the top and bottom quarks, respectively, give a contribution of the order of that of X_t, thus being quite relevant.

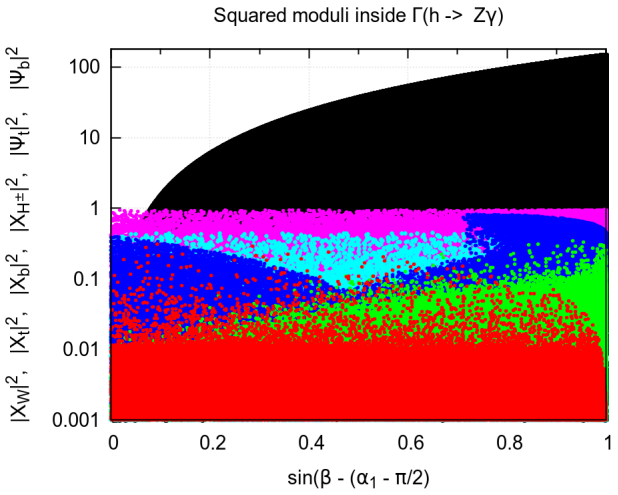

FIG 5. Points obeying bounded from below, perturbative unitarity and S, T, U constraints representing the squared moduli of $C\, Y_G$ (black), $k_U\, Y_{F\,\mathrm{top}}$ (blue), $k_D\, Y_{F\,\mathrm{bottom}}$ (red), $\lambda\, Y_H$ (green), Ψ_t (purple) and Ψ_b (cyan) as a function of $\sin(\beta - (\alpha_1 - \pi/2))$ for the Type II 2HDM.

ii. C2HDM Models

Fig. 6 shows our results in the $\mu_{\gamma\gamma} - \mu_{Z\gamma}$ plane for the Type I model. We notice that large pseudoscalar components (large $|s_2|$) imply small values for $\mu_{Z\gamma}$. There are two points to stress. First, there is a strong correlation between $\mu_{Z\gamma}$ and $\mu_{\gamma\gamma}$, even when all values of s_2 are taken into account. Second, that correlation is partly connected with s_2. This can be seen in the blue/black region of Fig. 7, where we see that large values of $\mu_{Z\gamma}$ are only possible around $s_2 \sim 0$ and h_1 with a large scalar component.

In contrast, a large pseudoscalar component implies very small values for both $\mu_{Z\gamma}$ and $\mu_{\gamma\gamma}$. As a result, a value of $\mu_{Z\gamma} \sim 1$ would be very efficient in ruling out a large pseudoscalar component. Fig. 7 also shows in

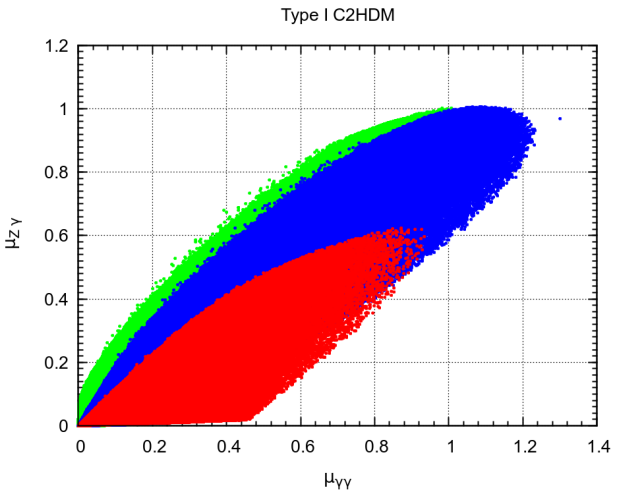

FIG 6. Results in the $\mu_{Z\gamma}$ - $\mu_{\gamma\gamma}$ plane for the Type I C2HDM. The points in green/light-gray, blue/black, and red/dark-grey correspond to $|s_2| < 0.1$, $0.45 < |s_2| < 0.55$, and $|s_2| > 0.85$, respectively.

red/dark-grey (cyan/light-grey) the allowed regions if we assume that the measurements of μ_{VV} at 14 TeV will center around unity with a 20% (5%) error. The VV constraint implies that $\mu_{\gamma\gamma}$ and $\mu_{Z\gamma}$ are expected to lie close to their SM value in the C2HDM and that $|\alpha_2|$ should lie below 50 degrees. A similar analysis of the impact of VV, shows that α_3 can take any value and that $|\alpha_1|$ should be larger than about 60 degrees.

We now consider the simulations for $Z\gamma$ in the Type II model, shown in Fig. 8. Large values for $\mu_{Z\gamma}$ are possible for small $|s_2|$. Comparing with Fig. 6, we see that, in Type II, much larger values of $\mu_{Z\gamma}$ (and of $\mu_{\gamma\gamma}$) are al-

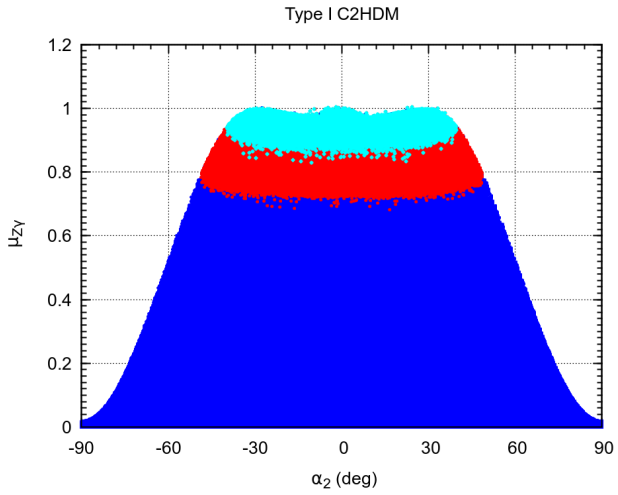

FIG 7. $\mu_{Z\gamma}$ as a function of s_2. The points in red/dark-grey (cyan/light-grey) where chosen to obey $\mu_{VV} = 1$ within 20% (5%). This figure has been drawn for 14 TeV.

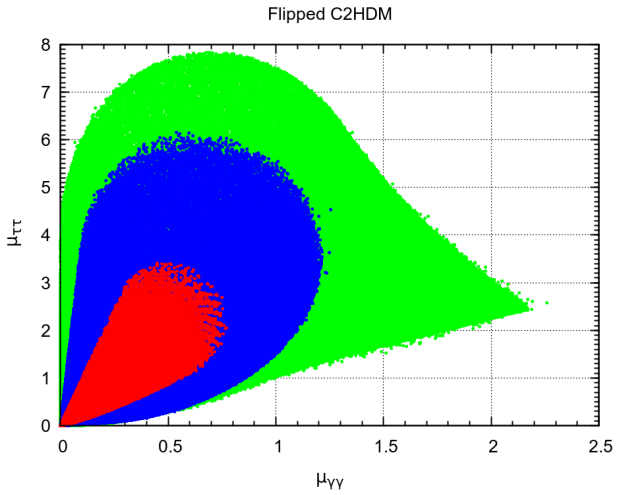

FIG 9. Flipped model results in the $\mu_{\tau^+\tau^-}$ - $\mu_{\gamma\gamma}$ plane. The points in red/dark-grey, blue/black, and green/light-gray correspond to $|s_2| < 0.1$, $0.45 < |s_2| < 0.55$, and $|s_2| > 0.85$, respectively.

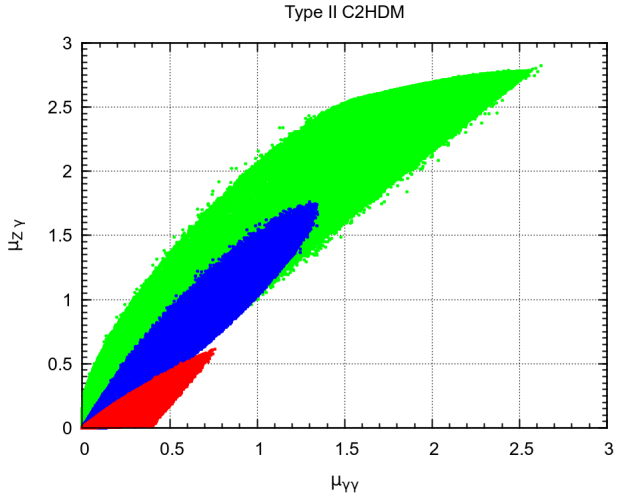

FIG 8. Type II results in the $\mu_{Z\gamma}$ - $\mu_{\gamma\gamma}$ plane. The points in red/dark-grey, blue/black, and green/light-gray correspond to $|s_2| < 0.1$, $0.45 < |s_2| < 0.55$, and $|s_2| > 0.85$, respectively.

lowed, but that there is still a strong correlation between the two which, again, is partly due to s_2. Measurements of μ_{VV} within 20% of unity, force $\mu_{Z\gamma} \sim 1$ and require $|\alpha_2| \lesssim 50$ degrees. This puts a further bound on a large pseudoscalar component.

In the Lepton Specific model, the results for $\mu_{Z\gamma}$ are very similar to those presented for Type I, while in the Flipped model, the results are similar to those of Type II.

We highlight the situation regarding $\mu_{\tau^+\tau^-}$ in the Flipped model, presented in Fig. 9. Notice that one can find points as large as $\mu_{\tau^+\tau^-} = 7.5$ for reasonable values of $\mu_{\gamma\gamma} \sim 1$.

iii. Wrong-sign $h_1 b\bar{b}$ couplings in Type II C2HDM

Here we discuss for the first time the wrong-sign $hb\bar{b}$ couplings in the context of the Type II C2HDM. We have seen that in the Type II real 2HDM we had $k_D = -\sin\alpha/\cos\beta$ (in fact, to be precise and independent of the phase conventions leading to the usual choices for the ranges of α, one should talk about $C\,k_D > 0$ as the right sign solution and $C\,k_D < 0$ as the wrong-sign solution).

The situation is rather different in the C2HDM because, according to Eq. (6), there are two couplings of h_1 with the fermions: the scalar-like coupling a and the pseudoscalar-like coupling b (so that we shall use the notation a_D and b_D for the couplings with the down-type quarks, and a_U and b_U for the couplings with the up-type quarks). As usual, we assume that experiments have obtained the SM values for μ_{ZZ}, μ_{WW}, $\mu_{\gamma\gamma}$, and $\mu_{\tau^+\tau^-}$ within 20%. Denoting by sgn(C) the sign of C, we show in Fig. 10 a simulation in the sgn(C) $\sin(\alpha_1 - \pi/2)$-$\tan\beta$ plane. In cyan/light-grey we show the points which pass $\mu_{VV} = 1.0 \pm 0.2$; in blue/black the points that also satisfy $|s_2|, |s_3| < 0.1$; and in red/dark-grey the points that satisfy $|s_2|, |s_3| < 0.05$. The left legs correspond to $\sin(\beta - \alpha) \sim 1$ and the right sign solution, while the right legs correspond to $\sin(\beta + \alpha) \sim 1$ and the wrong-sign solution. We see that, for generic s_2 and s_3, the two regions are continuously connected. In contrast, when $|s_2|, |s_3| < 0.05$, we tend to the disjoint solutions of the real 2HDM [26].

The constraints on the sgn(C) a_D-sgn(C) b_D plane are shown in Fig. 11. We see that sgn(C) a_D can have both signs, and so can sgn(C) b_D. Moreover, these different regions are continuously connected. In the C2HDM there is still a very large region of either negative sign permitted.

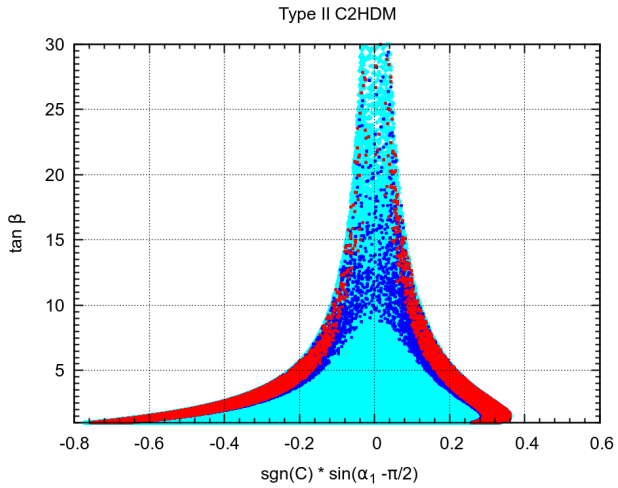

FIG 10. Results of the simulation of Type II C2HDM on the $\mathrm{sgn}(C)\sin(\alpha_1-\pi/2)$-$\tan\beta$ ($\sin\alpha$-$\tan\beta$) plane. In cyan/light-grey we show all points obeying $\mu_{VV}=1.0\pm0.2$; in blue/black the points that satisfy in addition $|s_2|$, $|s_3|<0.1$; and in red/dark-grey the points that satisfy $|s_2|$, $|s_3|<0.05$.

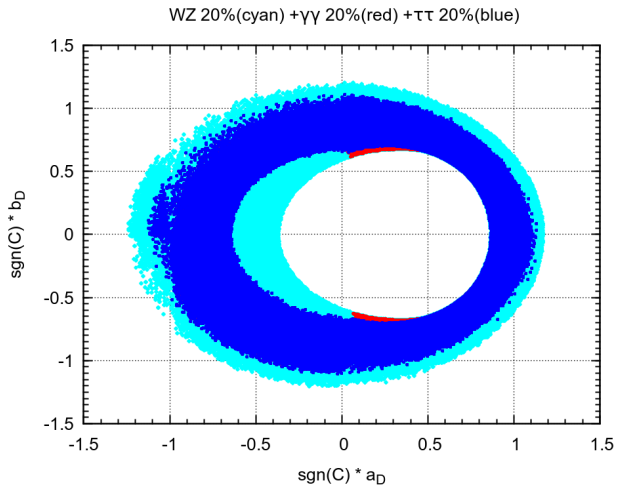

FIG 11. Results of the simulation of Type II C2HDM on the $\mathrm{sgn}(C)\,a_D$-$\mathrm{sgn}(C)\,b_D$ plane of scalar-pseudoscalar couplings of $h_1b\bar{b}$. We assume that the measurements come from current data at 8 TeV and are made within 20% (5%) of the SM. Constraints from μ_{VV} are in cyan/light-grey, from $\mu_{\gamma\gamma}$ are in red/dark-grey, and from $\mu_{\tau^+\tau^-}$ are in blue/black.

iv. Predictions in the 2HDM for the 14 TeV run

We now focus on the real 2HDM. Assuming current experiments (20% errors at 8 TeV) and, in addition, the μ_{VV} are measured at 14 TeV to lie around unity with a 5% precision, our predictions for $\mu_{Z\gamma}$ (in cyan/light-gray), $\mu_{\tau^+\tau^-}$ (in red/dark-gray) and $\mu_{\gamma\gamma}$ (in black) are shown in Fig. 12. Here, we would be led to conclude that a 5% measurement of $\mu_{\tau^+\tau^-}\sim1$ would exclude $k_D<0$ for large $\tan\beta$. As explained in Ref. [26], this conclusion is misleading since the $\mu_{\tau^+\tau^-}$ (and the $\mu_{b\bar{b}}$ rates, combining all production modes) depend crucially on the detailed mix of the gluon production through intermediate tops and bottoms. Thus, we agree with Ref. [22] that a 5% measurement of $\mu_{\gamma\gamma}$ can be used to exclude the wrong-sign solution, while $\mu_{\tau^+\tau^-}$ should not. Concerning $\mu_{Z\gamma}$, there are bad news and good news. The

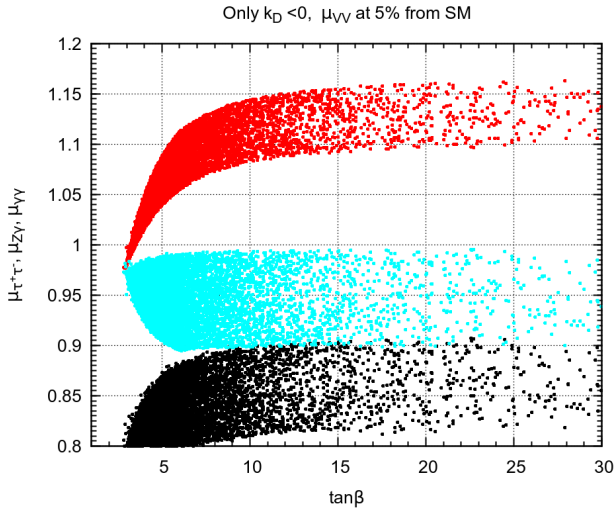

FIG 12. Prediction for $\mu_{\tau^+\tau^-}$ (red/dark-gray), $\mu_{Z\gamma}$ (cyan/light-gray) and $\mu_{\gamma\gamma}$ (black) as a function of $\tan\beta$, for the LHC at 14 TeV, with a measurement of μ_{VV} within 5% of the SM at 14 TeV.

bad news comes from the fact that the results in Fig. 12 show that $\mu_{Z\gamma}\lesssim1$. Therefore, this channel cannot be used to exclude the $k_D<0$ solution. The good news are the following. The ratio μ_{VV}, even at 20%, puts a strong bound on $\mu_{Z\gamma}$. In fact, we found that, for $k_D<0$ and before applying the μ_{VV} constraint, $\mu_{Z\gamma}$ could be as large as two for $\mu_{\gamma\gamma}\sim1$, as shown in the black region of Fig. 13. However, the requirement that μ_{VV} should be within 20% of the SM drastically limits this upper bound, requiring it to be very close to the SM value, as shown in the red/dark-gray region of Fig. 13. This means that a measurement of $\gtrsim1.3$ in $\mu_{Z\gamma}$ when $0.8<\mu_{VV}<1.2$ would exclude not only the SM but also the CP conserving 2HDM. If we require a measurement of μ_{VV} to be within 5% of the SM (cyan/light-gray region of Fig. 13), then both $\mu_{\gamma\gamma}$ and $\mu_{Z\gamma}$ have to be below their SM values for $k_D<0$. We find that this effect is more predominant in $\gamma\gamma$ ($\mu_{\gamma\gamma}<0.9$) than in $Z\gamma$ ($\mu_{Z\gamma}<1$).

V. CONCLUSIONS

We discuss the decay of a mixed scalar/pseudoscalar state into $Z\gamma$, which will be probed in the next LHC run. We consider the constraints that current experiments impose on the four versions of the C2HDM and discuss the

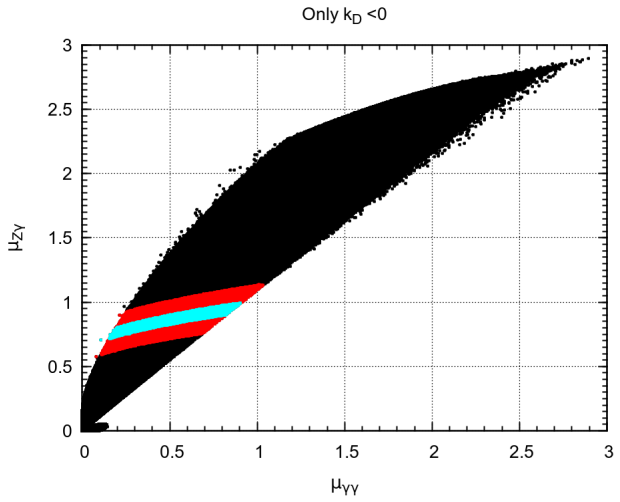

FIG 13. Predictions for $\mu_{Z\gamma}$ versus $\mu_{\gamma\gamma}$ at 14 TeV, for $k_D < 0$. In black, we have the points in the SET (obeying theoretical constraints and S, T, U, only). In red/dark-gray (cyan/light-gray), the points satisfying in addition VV within 20% (5%) of the SM, at 14 TeV.

prospects of future bounds, including $h \to Z\gamma$. This provides an update of Type I and Type II, and the first discussion of current constraints on the Lepton Specific and Flipped C2HDM.

In the C2HDM, the parameter s_2 measures the pseudoscalar content, with $s_2 = 0$ ($s_2 = 1$) corresponding to a pure scalar (pseudoscalar). The fact that ATLAS has a rather large central value for $\mu_{\gamma\gamma}$ places strong limits on C2HDM, but it also disfavours the SM at 2-σ. But, even excluding this constraint, we find that current experiments already disfavor a large pseudoscalar component $|s_2| > 0.85$, at over 1-σ level in all C2HDM versions.

We have discussed the possibility that the scalar component of the Type II C2HDM $h_1 q\bar{q}$ coupling (a) has a sign opposite to that in the SM. Current experiments allow for either sign of both $\mathrm{sgn}(C)\, a_D$ and $\mathrm{sgn}(C)\, b_D$, covering a rather large region.

Finally, we performed an analysis of $Z\gamma$ in the real 2HDM. We have shown that, before including the LHC data, values of $\mu_{\gamma\gamma}$ and $\mu_{Z\gamma}$ were allowed between 0 and 3, but with a correlation between the two, as shown in the black region of Fig. 13. Things change dramatically when the simple constraint $0.8 < \mu_{VV} < 1.2$ is imposed. In that case, we obtain the red/dark-gray region of Fig. 13, which already places $\mu_{\gamma\gamma}$ and $\mu_{Z\gamma}$ close to the SM. A 5% measurement of VV around the SM at 14 TeV will bring $\mu_{Z\gamma}$ just below unity. Thus, this decay cannot be used to exclude $k_D < 0$. But we have the reverse advantage. It is obvious that a measurement of $\mu_{Z\gamma} > 1$ would exclude the SM. We have shown that a 5% precision on μ_{VV} around the SM, together with $\mu_{Z\gamma} > 1$, would also exclude $k_D < 0$, and, together with $\mu_{Z\gamma} > 1.1$, would exclude altogether the Type II 2HDM with softly broken Z_2. If $\mu_{Z\gamma}$ turns out to lie a mere 20% above the SM value, then the softly broken Type II 2HDM is not the solution.

[1] G. Aad *et al.* [ATLAS Collaboration], Phys. Lett. B **716** (2012) 1 [arXiv:1207.7214 [hep-ex]].
[2] S. Chatrchyan *et al.* [CMS Collaboration], Phys. Lett. B **716** (2012) 30 [arXiv:1207.7235 [hep-ex]].
[3] T. Aaltonen *et al.* [CDF and D0 Collaborations], Phys. Rev. Lett. **109** (2012) 071804 [arXiv:1207.6436 [hep-ex]].
[4] T. Aaltonen *et al.* [CDF and D0 Collaborations], Phys. Rev. D **88** (2013) 5, 052014 [arXiv:1303.6346 [hep-ex]].
[5] [ATLAS Collaboration], ATLAS-CONF-2013-034.
The ATLAS collaboration, ATLAS-CONF-2013-072.
The ATLAS collaboration, ATLAS-CONF-2013-012.
[6] M. E. Chasco [CMS Collaboration], arXiv:1310.1002 [hep-ex].
CMS-PAS-HIG-13-005.
V. Khachatryan *et al.* [CMS Collaboration], arXiv:1407.0558 [hep-ex].
[7] S. Chatrchyan *et al.* [CMS Collaboration], Phys. Rev. D **89** (2014) 012003 [arXiv:1310.3687 [hep-ex]].
[8] B. Tuchming [CDF and D0 Collaborations], arXiv:1405.5058 [hep-ex].
[9] ATLAS collaboration. Talk given by Marumi Kado at ICHEP2014, July 2014, Valencia, Spain.
[10] CMS collaboration. Talk given by A. David at ICHEP2014, July 2014, Valencia, Spain.
[11] P. M. Ferreira, R. Santos, M. Sher and J. P. Silva, Phys. Rev. D **85** (2012) 077703 [arXiv:1112.3277 [hep-ph]].
[12] A. Barroso, P. M. Ferreira, R. Santos and J. P. Silva, Phys. Rev. D **86** (2012) 015022 [arXiv:1205.4247 [hep-ph]].
[13] A. Alves, E. R. Barreto and A. G. Dias, arXiv:1312.5333 [hep-ph].
[14] G. Aad *et al.* [ATLAS Collaboration], Phys. Lett. B **732** (2014) 8 [arXiv:1402.3051 [hep-ex]].
[15] S. Chatrchyan *et al.* [CMS Collaboration], Phys. Lett. B **726** (2013) 587 [arXiv:1307.5515 [hep-ex]].
[16] T. D. Lee, Phys. Rev. D **8** (1973) 1226.
[17] G. Aad *et al.* [ATLAS Collaboration], Phys. Lett. B **726** (2013) 88 [arXiv:1307.1427 [hep-ex]].
[18] S. Chatrchyan *et al.* [CMS Collaboration], Phys. Rev. D **89** (2014) 092007 [arXiv:1312.5353 [hep-ex]].
[19] D. Carmi, A. Falkowski, E. Kuflik and T. Volansky, JHEP **1207** (2012) 136 [arXiv:1202.3144 [hep-ph]].
[20] C. -W. Chiang and K. Yagyu, JHEP **1307** (2013) 160 [arXiv:1303.0168 [hep-ph]].
[21] A. Barroso, P. M. Ferreira, R. Santos, M. Sher and J. P. Silva, arXiv:1304.5225 [hep-ph], talk given by R. Santos at Toyama International Workshop on Higgs as a Probe of New Physics (13-16, February, 2013).
[22] P. M. Ferreira, J. F. Gunion, H. E. Haber and R. Santos, Phys. Rev. D **89** (2014) 115003 [arXiv:1403.4736 [hep-

ph]].
[23] A. Arhrib, E. Christova, H. Eberl and E. Ginina, JHEP **1104** (2011) 089 [arXiv:1011.6560 [hep-ph]].
[24] A. W. El Kaffas, W. Khater, O. M. Ogreid and P. Osland, Nucl. Phys. B **775** (2007) 45 [hep-ph/0605142].
[25] D. Fontes, J. C. Romão and J. P. Silva, arXiv:1408.2534 [hep-ph].
[26] D. Fontes, J. C. Romão and J. P. Silva, Phys. Rev. D **90** (2014) 015021 [arXiv:1406.6080 [hep-ph]].
[27] N. G. Deshpande and E. Ma, Phys. Rev. D **18** (1978) 2574.
[28] I. F. Ginzburg and I. P. Ivanov, hep-ph/0312374.
[29] M. E. Peskin and T. Takeuchi, Phys. Rev. Lett. **65** (1990) 964.
[30] M. E. Peskin and T. Takeuchi, Phys. Rev. D **46** (1992) 381.
[31] R. Mertig, M. Böhm and A. Denner, *Feyn Calc - Computer-algebraic calculation of Feynman amplitudes*, *Comput. Phys. Commun.* **64** (1991) 345. See http://www.feyncalc.org.